

Development of cryogenic permanent undulators operating around liquid nitrogen temperature

T Tanaka^{1,5}, T Hara¹, T Bizen², T Seike², R Tsuru¹, X Marechal²,
H Hirano³, M Morita³, H Teshima³, S Nariki⁴, N Sakai⁴,
I Hirabayashi⁴, M Murakami⁴ and H Kitamura¹

¹ RIKEN SPring-8 Center, 1-1-1 Koto, Sayo, Hyogo 679-5148, Japan

² Japan Synchrotron Radiation Research Center, 1-1-1 Koto, Sayo, Hyogo 679-5198, Japan

³ Nippon Steel Co. Ltd., 20-1 Shintomi, Futtsu, Chiba 293-8511, Japan

⁴ International Superconductivity Technology Center, 1-10-13 Shinonome, Koto-ku, Tokyo 135-0062, Japan

E-mail: ztanaka@spring8.or.jp

New Journal of Physics **8** (2006) 287

Received 5 July 2006

Published 28 November 2006

Online at <http://www.njp.org/>

doi:10.1088/1367-2630/8/11/287

Abstract. The cryogenic permanent magnet undulator (CPMU) is an insertion device in which permanent magnets (PMs) are cooled to a cryogenic temperature to improve magnetic performances in terms of remanence and coercivity. Operation of CPMUs is expected to be much easier than that of existing superconductive undulators (SCUs) with low-temperature superconducting coils, since the operating temperature can be much higher than that of liquid helium. In addition to pure PMs, high-permeability pole pieces and/or high-temperature superconductors (HTSCs) can be exploited to enhance the magnetic field of the CPMU. Towards realization of this concept, a number of R&Ds are in progress at SPring-8: field measurement under a cryogenic environment and reinforcement of HTSC samples. Encouraging results have been obtained from preliminary studies.

⁵ Author to whom any correspondence should be addressed.

Contents

| | |
|---|-----------|
| 1. Introduction | 2 |
| 2. Possible designs for CPMUs | 3 |
| 3. Radiation damage of PMs at low temperatures | 5 |
| 4. Preliminary studies on CPMU of pure type | 6 |
| 4.1. CPMU prototype | 6 |
| 4.2. Gap monitoring system | 6 |
| 4.3. Field measurement apparatus | 7 |
| 4.4. Measurement procedure | 7 |
| 4.5. Results of measurement | 8 |
| 4.6. Discussion | 10 |
| 5. Preliminary study on CPMU of HTSC type | 10 |
| 5.1. Reinforcement of the ring HTSC | 11 |
| 5.2. Methods of reinforcement | 11 |
| 5.3. Experiments | 11 |
| 5.4. Discussion | 15 |
| 6. Summary and outlook | 15 |
| Acknowledgments | 16 |
| References | 16 |

1. Introduction

Now-a-days, it is commonly believed that undulators are powerful tools for synchrotron radiation (SR) science because the undulator radiation has good coherence properties and a very small volume in the transverse phase space so that much higher brightness may be obtained compared to conventional bend sources. The most important issue in undulator development is to obtain a shorter period with higher magnetic field. Therefore, it seems to be natural to utilize superconducting technology to realize the above condition. In fact, the first undulator installed in a storage ring was of superconductive type operating at 4 K (superconductive undulator (SCU)). This undulator, of vertical type with the periodic length of 4 cm, was installed in the storage ring at L.U.R.E. in 1979 [1]. Although the vacuum gap, the inner height of the vacuum duct, was 12 mm, the magnetic gap was so wide as 22 mm because of the existence of a thermal shield. As a result, the magnetic field attained was not so high compared to that of a permanent magnet undulator (PMU) proposed later [2]. The minimum magnetic gap of the PMU was 15 mm and the magnetic field for the same period was expected to be 0.6 T higher than that of the SCU, that is the reason why development of the SCUs had been stopped for a long time until a new SCU design of in-vacuum type was proposed in 1998 [3]. Therefore, we can say that the essential point to obtain high magnetic field for short-period undulators is how to reduce the magnetic gap.

In 1990, the first in-vacuum undulator (IVU) was operated in the storage ring at KEK (High Energy Accelerator Research Organization) [4]. This undulator had no vacuum duct in the magnetic gap since the magnet arrays were located in the vacuum. Therefore, the magnetic gap width could be reduced to an ultimately small value without losing the electron beam. Based on the design of the above first IVU, numerous IVUs amounting to twenty have been constructed and

installed at SPring-8 [5]. In 1997, furthermore, a special IVU with a very short period of 11 mm was installed and successfully operated in the NSLS (National Synchrotron Light Source) ring at BNL (Brookhaven National Laboratory) in collaboration with SPring-8 [6], which demonstrated that high brightness x-rays could be obtained with IVUs even in medium-scale facilities.

The IVU design has brought popularization of high brightness x-rays as well as a new concept on medium scale SR facilities [7]. A combination of IVUs and a low emittance ring with a moderate beam energy may realize a moderate-cost and medium-sized SR facility having a performance comparable to that of the existing large-scale facilities. Most of the medium scale facilities such as SLS (Swiss), DIAMOND (UK), SOLEIL (France), SSRF (China), AS (Australia) are thought to be based on the above concept.

Although the design of IVUs enables a short magnetic gap, there is a crucial limit in the performance of PM material, NdFeB currently adopted for undulators. The theoretical limit of remanence of NdFeB is about 1.6 T [8]. PM material with high coercivity is required for the IVUs in order to avoid demagnetization during vacuum bakeout at a high temperature above 370 K for realizing ultrahigh vacuum. Considering that PM material with high remanence has low coercivity, we should adopt PM material with remanence lower than 1.3 T, which gives the performance limit in IVUs. Therefore, we have to adopt alternative designs to obtain higher magnetic performance than that of IVUs.

At present, there are two different approaches. One is to adopt SCUs based on a new design. Differently from the first SCU at L.U.R.E., the design must be of cold-bore type or in-vacuum type [9]. The cold surface at 4 K may suffer heat load from the electron beam or SR. Taking into account that a cooling capacity of a compact cryocooler is only 2 W at 4 K, the most important issue is how to overcome such a thermal budget problem. The other approach is to adopt cryogenic PMUs (CPMUs) proposed at SPring-8 in 2004 [10], which will be operated at a temperature ranging from 50 to 150 K. The principle of the CPMU is as follows. The remanence and coercivity of NdFeB PMs show negative temperature dependence as -0.1 and $-0.6\% \text{ K}^{-1}$, respectively [11]. Therefore, we can expect at a cryogenic temperature much higher undulator performance as well as much higher resistance against radiation damage. Development of the CPMU is straight forward from the current IVU and there is no big technological obstruction. Differently from SCUs, furthermore, heat load problem is negligible because we can expect much higher cooling capacity of cryocooler, for example, 200 W at 77 K. In this paper, the status of the CPMU development at SPring-8 is described.

2. Possible designs for CPMUs

The CPMU concept is easily realized by a slight modification of the design of existing IVUs. What is necessary is to install components to cool down the magnet arrays and control the temperature. In addition, the PM material should be replaced with that having high remanence (and accordingly low coercivity) at room temperature (RT). Operating the PM arrays at a cryogenic temperature, both the remanence and coercivity are significantly improved, resulting in a much higher magnetic performance than those in existing IVUs. In addition to the simple design for CPMUs described above, two different designs have been proposed to date: hybrid type [10] and high-temperature superconductor (HTSC) type [12]. Schematic illustrations of possible designs for CPMUs are shown in figures 1(a)-(c).

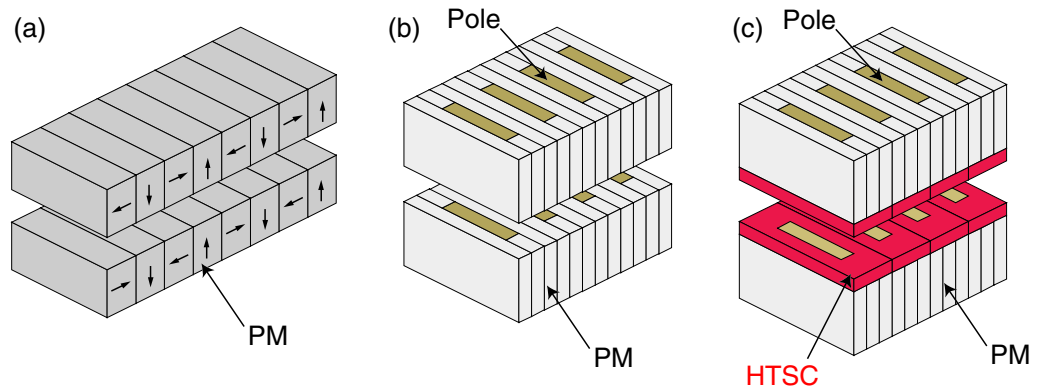


Figure 1. Possible designs for CPMUs: (a) pure type, (b) hybrid type and (c) HTSC type.

Table 1. Comparison of magnetic performances for various undulator types.

| Undulator type | Peak field (T) | PM material |
|---|----------------|-------------|
| IVU | 0.67 | NEOMAX35EH |
| SCU | 1.30 [9] | None |
| CPMU pure | 0.93 | NEOMAX50BH |
| CPMU hybrid | 1.10 | NEOMAX50BH |
| CPMU HTSC type ($j_c = 1 \text{ kA mm}^{-2}$) | 1.30 | NEOMAX53CR |
| CPMU HTSC type ($j_c = 2 \text{ kA mm}^{-2}$) | 1.50 | NEOMAX53CR |

In the hybrid type (figure 1(b)), pole pieces made of high-permeability material such as vanadium permendur are inserted as a flux concentrator. Operation at a cryogenic temperature gives us a possibility to use material with a saturation field higher than that of permendur such as dysprosium having a saturation field of 3.2 T at 77 K.

In the HTSC type (figure 1(c)), ring-shaped bulk HTSCs (ring HTSCs) are mounted on the hybrid magnet arrays. The ring HTSCs are magnetized in order to keep the magnetic flux inside when the gap is opened from 0 to a nominal value. The operating temperature should be at least lower than the critical temperature of the HTSC material. For more details of the principle of this concept, refer to [12].

Table 1 shows a comparison between the conventional IVU, existing SCU, and three types of CPMUs. The periodic length and gap value are assumed to be 14 and 5 mm, respectively. It should be noted that the performance of the HTSC type is sensitive to the critical current density (j_c) of the HTSC material to be adopted. Here, calculation results for two typical j_c values are indicated. HTSCs with j_c of 1 kA mm^{-2} are available with the state-of-the-art technology in the HTSC industry but we need more scientific investigations and technical innovations for a practical use of HTSCs with j_c higher than this value. It is worth noting, however, that the performances of HTSCs are being improved year by year [13]–[17]. The HTSCs with j_c higher than, e.g. 2 kA mm^{-2} will be very possible to be available in the near future.

As mentioned in [10], the PM materials suitable for CPMUs are NEOMAX-50BH and -53CR (NEOMAX Co., Ltd.). The 50BH material shows the best magnetic performance, the remanent field of 1.6 T and the coercivity of 3000 kA mm^{-1} , at 140 K. Below this temperature,

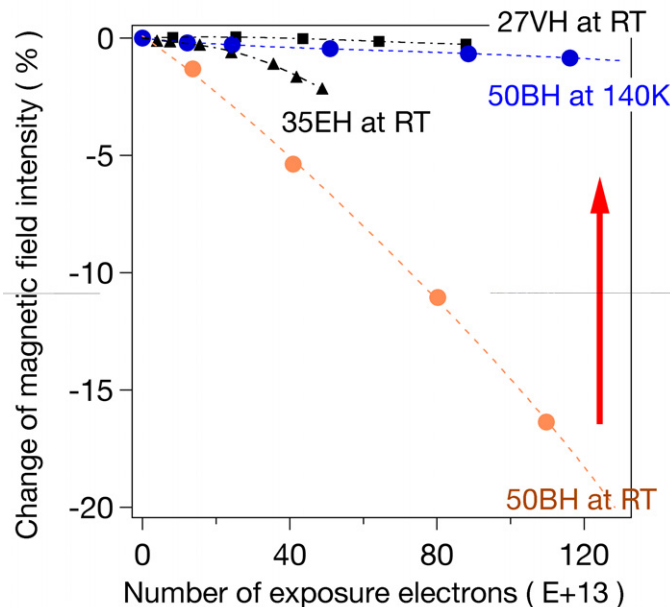


Figure 2. Results of experiments to measure the radiation damage for various PM material.

however, the remanent field decreases due to the spin reorientation. On the other hand, the remanence of 53CR (PrFeB), different material from conventional NdFeB shows monotonic increase at low temperatures with a typical field higher than 1.5 T below 77 K. Therefore, 53CR is the best choice for the CPMUs of HTSC type or hybrid type with dysprosium poles, and 50BH for pure type or hybrid type with permendur poles.

Because of the low coercivity at RT, it is not allowed to bake out the magnet arrays made of 50BH or 53CR. Because the amount of outgass from the magnet arrays is significantly reduced at a cryogenic temperature, it is expected that the achievable pressure will be much better than that at RT. However, we need a careful investigation on the vacuum system for CPMUs to ensure compatibility to the accelerator vacuum system. In addition, the cooling system should be very reliable. In case of failure of the cooling system, the accelerator operation should be stopped, otherwise the PMs may be damaged due to radiation. One solution to this problem is to install more than one cryocoolers. Even if one of them is broken, the remaining cryocoolers can cool the PMs to avoid demagnetization. In this case, the gap may have to be opened to reduce the heat load as much as possible, meaning that operation of the device may not be allowed until the broken cryocooler is repaired.

3. Radiation damage of PMs at low temperatures

In the previous study [18], it was found that PMs with high coercivity tend to have high resistance against radiation damage. Furthermore, NdFeB PMs show high coercivity at a low temperature as mentioned above. Therefore, PMs cooled to a cryogenic temperature are expected to show high radiation resistance. To confirm this possibility, we studied radiation damage of 50BH PM material using the 2 GeV electron LINAC at Pohang Light Source. Figure 2 shows the radiation damage of 50BH PM at different temperatures in comparison to 27VH and 35EH at RT. The

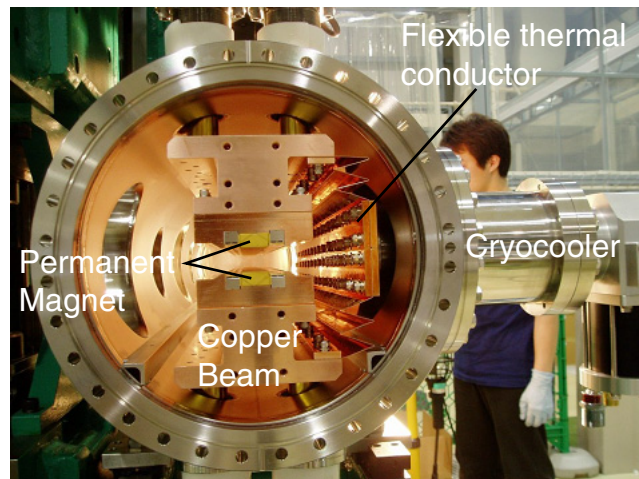


Figure 3. Photograph of the cryoundulator prototype. Except the components for cooling, the structure is the same as the existing IVUs.

radiation damage at RT is serious, however, the damage at 140 K is comparable to that of 27VH (NEOMAX Co., Ltd.) at RT and smaller than that of 35EH (NEOMAX Co., Ltd.) at RT. Taking into account that 27VH and 35EH PMs are used routinely for IVUs, cooled 50BH can be used for CPMUs as high radiation resistant material.

4. Preliminary studies on CPMU of pure type

4.1. CPMU prototype

The cryoundulator concept can be realized by a simple modification of existing IVUs. It should be noted, however, that a field correction technique applicable to magnet arrays in a cryogenic environment should be established. In other words, a thorough study of magnetic properties of the magnet array at a cryogenic temperature is required. We constructed a cryoundulator prototype by modification of an existing IVU and measured the magnetic field to investigate the dependence of the magnetic property on temperature in terms of the error distribution as well as the field strength.

Figure 3 shows a photograph of the cryoundulator prototype. The length of the device (vacuum chamber and mechanical frame) is about 1500 mm, while the magnet length is 600 mm. The periodic length is 15 mm at RT, resulting in 40 periods. NEOMAX50BH (NEOMAX Co. Ltd.) has been employed as PM material. In-vacuum beams holding the magnet arrays are made of copper for better thermal conductivity, and are supported by rods made of stainless steel. A flexible thermal conductor made of copper has been installed to connect the copper beam and cryocooler. Temperatures of the magnet array can be monitored with platinum resistance thermometers (PT100) attached to the magnet units. In addition, sheath heaters have been installed for temperature control.

4.2. Gap monitoring system

It is expected that the gap value is varied due to thermal contraction of the supporting rods during the cooling process. This gap variation should be compensated for precise measurement of the

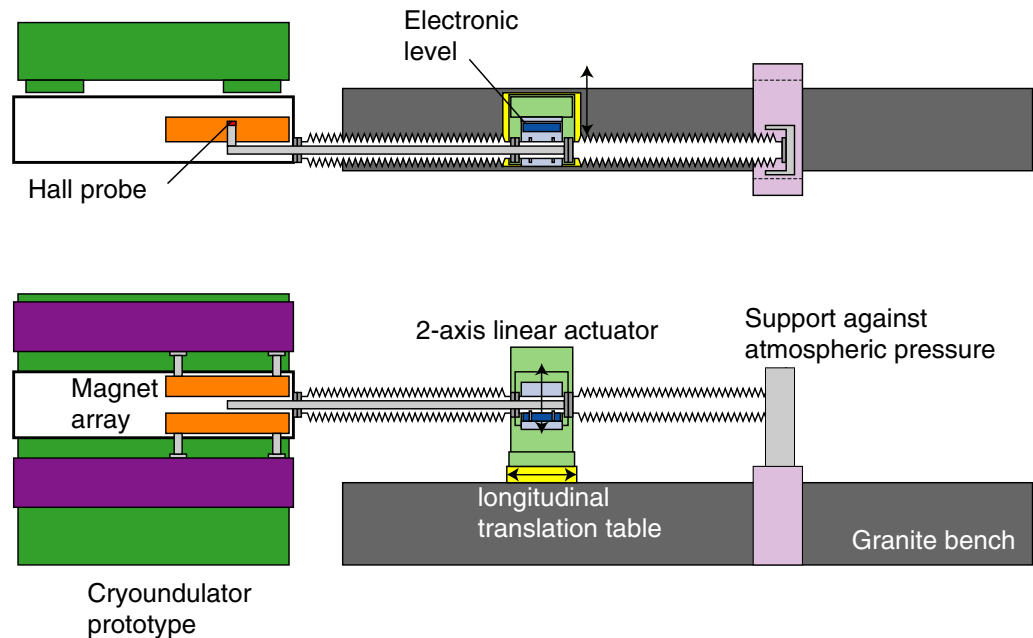


Figure 4. Schematic illustration of the apparatus developed for field measurement of the cryoundulator prototype.

magnetic field. Capacitance-type displacement monitors (Nanotex Corp.) have been used for this purpose. Two displacement monitors were placed on both sides of a ceramic plate with a thickness of 2 mm in order to measure the gap between two conductive objects. Two sets of the gap monitors were installed upstream and downstream to obtain an average of the gap value. In addition, gap taper could be evaluated by subtraction of the two gap values.

4.3. Field measurement apparatus

Figure 4 shows a schematic illustration of the field measurement apparatus developed for field measurement of the cryoundulator prototype. The Hall probe was placed on the in-vacuum cantilever fixed in the vacuum tube that was connected to the 2-axis linear actuator. Two bellows with a stroke length of 600 mm were installed. One was to ensure a free translation of the cantilever in vacuum and was inserted between the end of the undulator chamber and the vacuum tube in which the cantilever was fixed. The other was installed on the opposite side to avoid unwanted stress due to the atmospheric pressure. The 2-axis actuator was supported by the linear-translation table placed on the granite bench with a high mechanical precision. The transverse position of the Hall probe was determined by the 2-axis actuator, while the linear-translation table was used to scan the Hall probe in the longitudinal (undulator axis) direction.

4.4. Measurement procedure

The field measurement was performed at temperatures of 293, 253, 213, 173, 133 and 93 K (RT). In order to set the temperature of the magnet array to the above values, temperature controllers were used to adjust the current in the sheath heater. After the temperature was stabilized, the gap was adjusted exactly to 4 mm with the gap variation taken into account. Then the magnetic-field

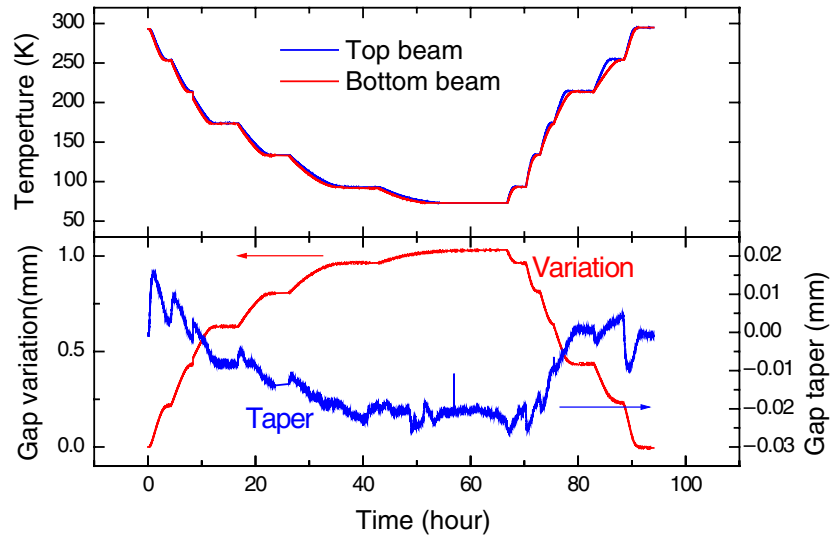


Figure 5. Temperature and gap variation during the experiment. Top panel: temperatures measured at the top and bottom magnet arrays. Bottom panel: gap variation and taper measured with the capacitance-type displacement monitor.

distribution was measured by scanning the Hall probe in the longitudinal direction. During the longitudinal translation, it was found that the cantilever was tilted by a mechanical stress due to the bellows movement: it worked as a spring when it expanded or shrank. In order to overcome this difficulty, we measured the tilt angle by an electronic level placed on the vacuum tube on the 2-axis actuator, and made a feedback on the vertical position of the Hall probe.

4.5. Results of measurement

4.5.1. Gap variation. Figure 5 shows the temperature of the magnet array, and the gap variation and taper as functions of time after the cryocooler was turned on. It took about 20 h to reach 133 K. The gap was found to become wider as the temperature was reduced, which was a consequence of thermal contraction of the supporting rods. In addition, the gap was tapered slightly during the cooling process, which was probably due to difference in thermal contraction between supporting rods located downstream and upstream. In order to check the reproducibility, the gap variation and taper are plotted as functions of the magnet temperature in figure 6. The red and blue lines show the results for the cooling and heating processes, respectively. The dotted lines indicate the temperatures where the field measurement was performed. Considering the fact that the system was in a steady state only at these temperatures, we can say that the gap values are reproducible.

4.5.2. Magnetic properties. Figure 7 shows the peak field averaged over the central 70 poles as a function of the temperature. At 133 K, the magnetic field was found to be increased by 14% compared to that at (RT). This value is slightly higher than that (10%) obtained for a single PM block [10], the reason for which is unknown. One possible reason is a difference in permeance coefficient between the single piece and magnet assembly.

Besides the increase of the peak field, we have to take care of the variation of the field distribution due to temperature change. Figure 8 shows the phase error calculated from the

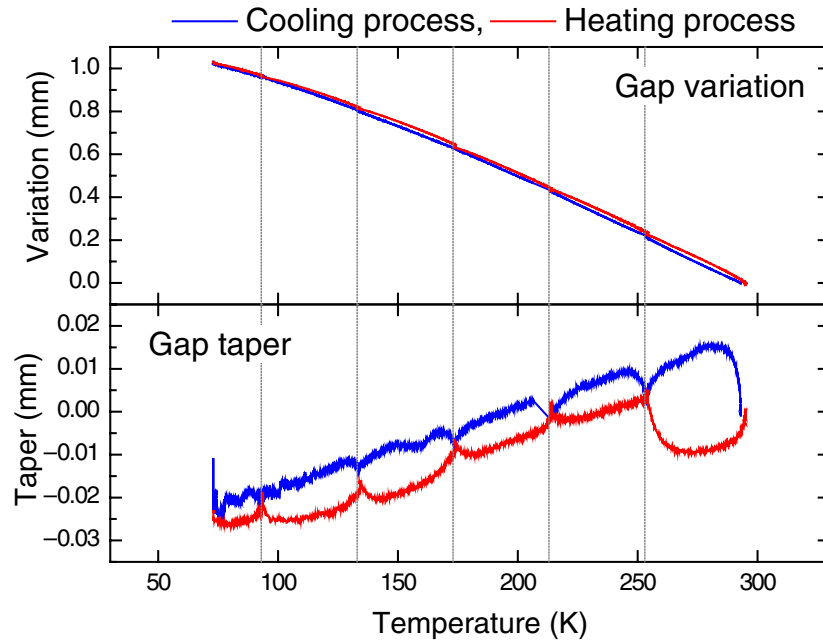


Figure 6. Reproducibility of the gap variation (top panel) and tapering (bottom panel) at different temperatures.

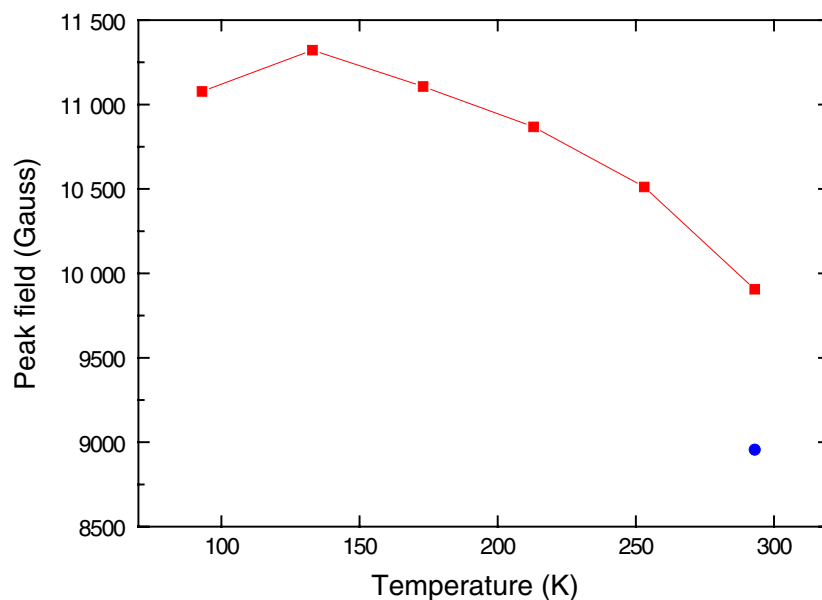


Figure 7. Peak field as a function of the temperature. The blue dot shows a theoretical value of the undulator peak field with the same periodic length (15 mm) and gap (4 mm) but the remanence of 1.15 T (NEOMAX35EH, NEOMAX Co. Ltd.)

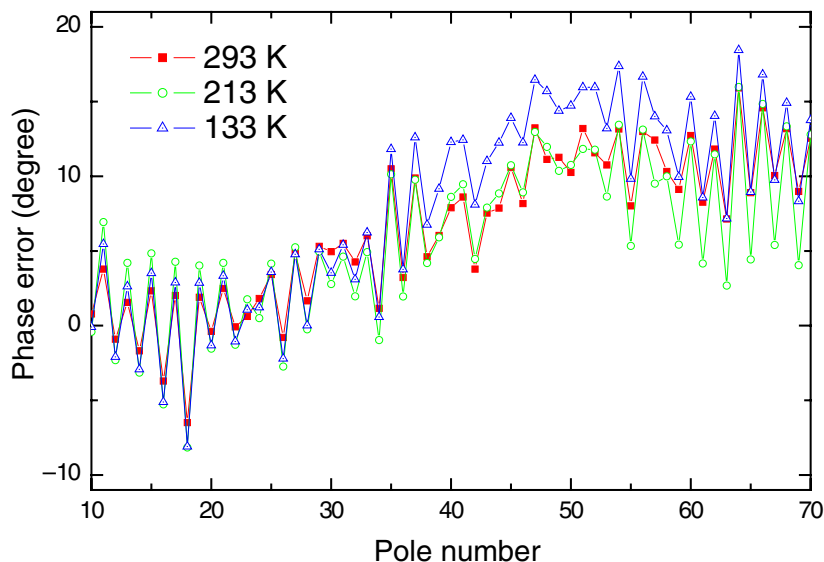


Figure 8. Phase error as a function of the pole number calculated from the magnetic field distribution measured at different temperatures.

measured field distribution as a function of the pole number at three different temperatures: 133, 213 and 293 K. We find no significant difference between them.

4.6. Discussion

The experimental result described in the preceding section suggests that the magnetic error distribution is not sensitive to temperature variation. This is a very encouraging result with respect to the field correction procedure. We can apply a conventional field correction procedure to reduce the phase error not only at RT but also at a cryogenic temperature. It should be noted, however, that the cryoundulator prototype used in this experiment only contains PMs as magnetic material. In fact, high-permeability material such as permendur will be employed as pole pieces to get higher field. In such a case, the temperature coefficient of the pole piece material may have some influence on the error distribution.

5. Preliminary study on CPMU of HTSC type

Towards realization of the HTSC-type CPMU (hereinafter, cryoundulator plus), we have a lot of technical challenges to overcome. The magnetic reproducibility of the HTSCs should be within some criterion so that the photon flux available on the samples does not vary significantly during experiments. The criterion may be more severe for larger number of undulator periods and higher harmonic numbers. In addition, a field correction procedure should be established so as to reduce the optical phase error and multipole components. The temperature stability and uniformity along the undulator are also crucial because the critical current density of superconducting material, which determines the magnetic performance, is strongly dependent on temperature. Besides these points, what is the most important is the mechanical stability of the ring HTSCs.

5.1. Reinforcement of the ring HTSC

During the proof-of-principle experiments of the cryoundulator plus [12], it was found that the magnetic performances of the ring HTSCs degraded. In the worst case, the ring HTSC sample completely lost the superconducting property and no field enhancement was observed after several trials. In order to investigate the reason, the spatial profile of the magnetic field generated by the ring HTSC was measured by scanning a Hall probe under application of a uniform external field [19]. At a low external field, a typical profile generated by a single current loop was observed, while it changed to a hollow one when the strength of the external field increased. By analysing the profile, it was verified that several local current loops were created in the HTSC sample and that the ring HTSC was damaged mechanically. Thus it is indispensable to improve the mechanical property of the ring HTSC for realization of the cryoundulator plus. We have so far tested two procedures to reinforce the ring HTSC.

5.2. Methods of reinforcement

5.2.1. Resin impregnation. When a large-sized single grain bulk HTSC (typically with a diameter of several cm) is strongly magnetized, it can easily be broken due to an outward pressure produced by the persistent current and trapped magnetic field. Usually, cylindrical HTSC samples are reinforced with metal rings with an inner diameter same as the diameter of the HTSC sample. When the sample is cooled, it is compressed owing to a difference in thermal contraction between the metal ring and HTSC sample. It should be noted, however, that this method can be applied only to samples with a cylindrical shape, which is not the case for the ring HTSCs for the cryoundulator plus: in general, the width of the ring HTSC should be much longer than the length (half period) for better field uniformity along the horizontal axis. Instead, a resin impregnation technique, which is also an effective method for reinforcement of HTSC samples [15], can be applied. In this method, the sample is immersed in molten resin where the resin penetrates into a bulk superconductor through microcracks having openings on the surface. The voids connected to these cracks are also filled with resin, which drastically improves the mechanical properties of the HTSC samples.

5.2.2. Pole piece insertion. In addition to the resin impregnation described above, a pole piece made from high-permeability material such as permendur can be inserted and glued to the ring HTSC. In this case, the pole piece has two roles: one is a rib to support the hollow structure and the other is a flux concentrator to achieve stronger magnetic field (hybrid-undulator configuration). It is effective to use the resin impregnation to glue the pole piece and ring HTSC. What is a problem in this scheme is the difference in thermal expansion coefficient. Simple calculation shows that difference of contraction between the permendur and YBaCuO, a typical HTSC material, is around several microns when the temperature is reduced from 300 to 100 K, which may damage the glue function of the resin impregnation.

5.3. Experiments

In order to investigate the effects of the methods of reinforcement proposed in the preceding sections, we prepared several ring HTSC samples that were reinforced with several different methods and carried out experiments to check the mechanical property of these samples.

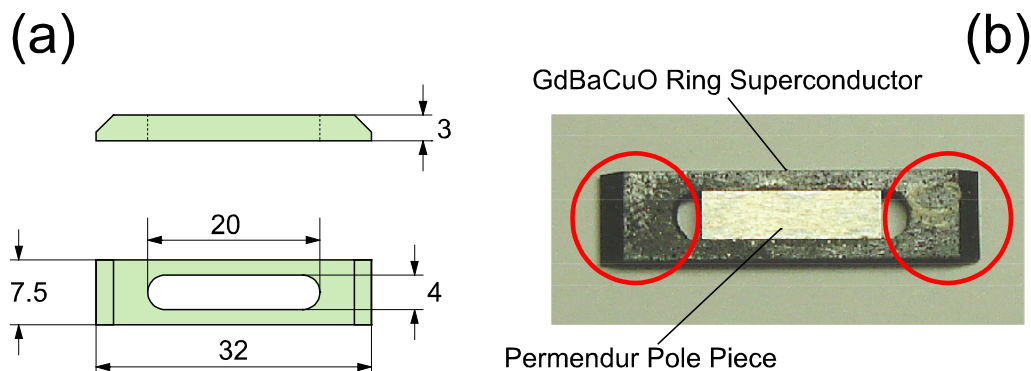


Figure 9. Right panel: overall dimensions of the ring HTSC sample prepared for the experiments to check the reinforcement method. Left panel: photograph of the sample C, in which a pole piece made of permendur is inserted.

5.3.1. Sample preparation. We prepared four ring HTSC samples (A, B, C and D) made of GdBaCuO. Figure 9(a) shows the overall dimensions of the sample. After machining, three samples (B, C and D) were immersed in epoxy resin for impregnation, where a pole piece made from permendur was inserted into the samples C and D. Thus the samples C and D have the same structure. No treatment was made for the sample A. Figure 9(b) shows a photograph of the sample C.

5.3.2. Experimental setup. The experimental setup is schematically shown in figure 10. The sample was fixed on a copper plate connected to the cryocooler head, and inserted into the gap of the electromagnet (normal conducting). A cartridge-type heater was installed on the copper plate to control the temperature. From the opposite side, the Hall probe fixed on the cantilever was inserted to measure the magnetic field. The cantilever was connected to the 2-axis linear actuator to scan the Hall probe and measure the spatial profile of the magnetic field. The temperature of the ring HTSC was measured with a platinum resistance thermometer (PT100). After cooling the sample to 25 K, the current of the electromagnet was increased gradually. At several values of the electromagnet current, the spatial profile of the magnetic field generated by the ring HTSC was measured. It should be noted that the electromagnetic stress in this case causes an inward pressure, which is opposite to the situation in the cryoundulator plus. We took this procedure just for simplicity of experiments. Nevertheless, this method suffices to check the mechanical property of the ring HTSC and its improvement by the reinforcement method described above. Using the sample C, we made experiments with the opposite condition, i.e., with an outward pressure generated during the magnetization process of the ring HTSC, which is explained in detail in the following sections.

5.3.3. Result. Figure 11 shows the results of the field-profile measurement for different values of the external field generated by the electromagnet (B_{ext}) in the case of the sample A (no treatment for reinforcement). For clarity, the magnetic field is subtracted by the value of the applied field by the electromagnet to show the net value generated by the ring HTSC itself (B_{sc}). Up to 1.6 T, a typical profile generated by a single current loop was observed. At $B_{\text{ext}} = 1.8$ T, however, the profile suddenly changed to a hollow one, meaning that the sample was broken.

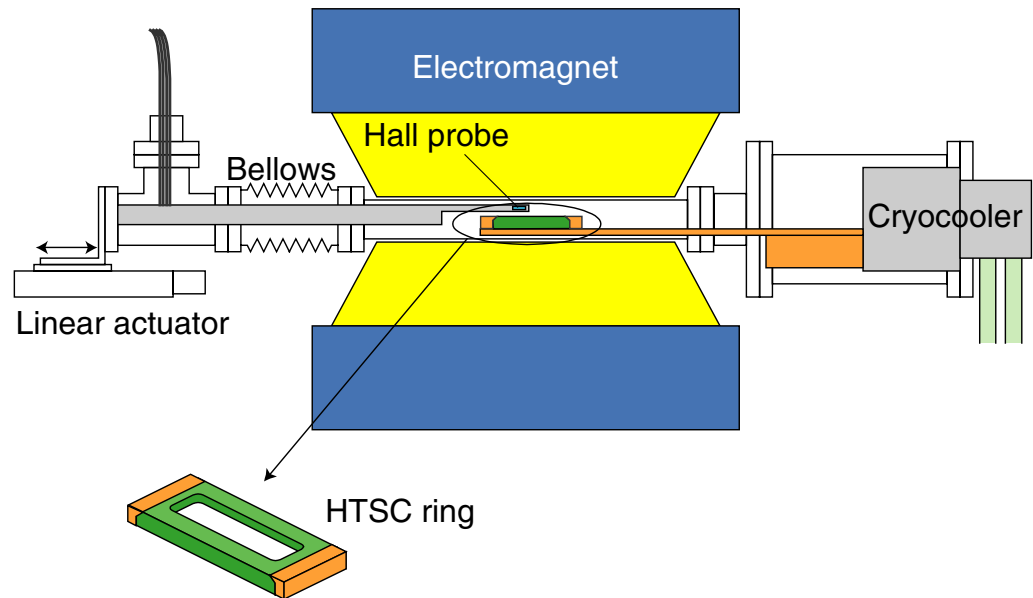


Figure 10. Experimental setup. The HTSC ring is mounted on a copper plate attached to the cryocooler head to be cooled down to 25 K and inserted in the gap of an electromagnet that can apply an uniform magnetic field of up to 2.0 T. A hall probe mounted on a cantilever is inserted from the opposite side to measure the magnetic field generated by the HTSC ring.

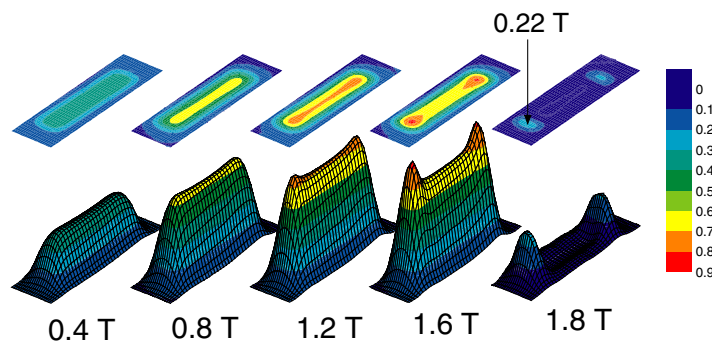


Figure 11. Spatial profiles of the magnetic field generated by the HTSC ring sample A (no treatment for reinforcement) for different values of the external field strength applied by the electromagnet. See text for details.

It is worth noting that two peaks of magnetic field were found when B_{ext} was higher than 1.6 T and that they remained even after the ring HTSC sample was broken. Paying attention to the geometrical structure of the ring HTSC shown in figure 9(b), we can conclude that the two peaks were generated by local current loops in the sections indicated by the red circles.

Figure 12 shows the results for the sample B, in which profiles similar to the sample A were observed, and it was found that the sample was broken at $B_{\text{ext}} = 1.6$ T. Thus the resin impregnation is not enough for reinforcement of the ring HTSC for realization of cryoundulator plus.

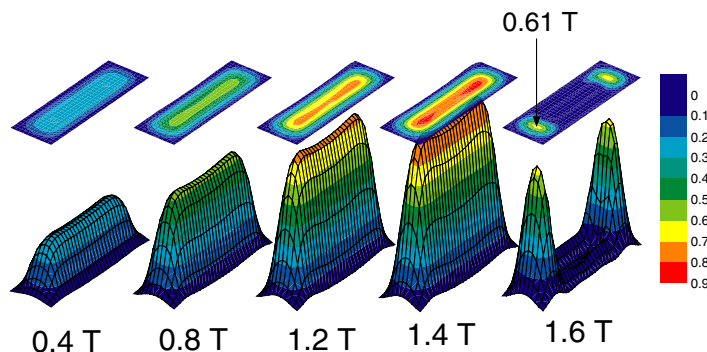


Figure 12. Spatial profiles of the magnetic field generated by the HTSC ring sample B (resin impregnation performed).

It should be noted that the peak field, which was generated by the local current loop after the sample B was broken, reached 0.61 T as indicated in figure 12. This is about three times larger than that of the sample A (0.21 T). This means that the critical current density of the sample B is much higher than that of the sample A. Such a large discrepancy was not found in the examination of the samples carried out independently at a temperature of liquid nitrogen (77 K). Two reasons can be considered: one is difference in the temperature dependence of the critical current density, and the other is the effect due to the resin impregnation. But we have not yet found the real reason.

We repeated the experiments with respect to the samples C and D and found that they survived even after B_{ext} reached 2.0 T, which was the maximum magnetic field generated by the electromagnet due to saturation of the iron yoke and lack of cooling capability. The experimental results are summarized in figure 13, in which B_{sc} at the central position of the ring HTSC is plotted as a function of B_{ext} .

Although both the samples C and D survived after applying the maximum field, the magnetic field performances are different significantly. The sample C reached saturation at $B_{\text{ext}} = 1.6$ T, while the sample D did not reach saturation even at $B_{\text{ext}} = 2.0$ T. Also, the initial slope at lower values of B_{ext} is different. These facts show that the deviation of the magnetic performance of the ring HTSC used in the experiment was not small.

After verification of the effects due to the reinforcement methods described previously, we carried out another experiments using the sample C. In this experiment, the procedure was the same as that described so far, but the initial condition was different. A magnetic field of 2.0 T was applied before the ring HTSC was cooled, then after it reached 25 K, the field of the electromagnet was decreased gradually and the magnetic profiles were measured at several values of B_{ext} . In this case, the ring HTSC was magnetized with the same polarity as the electromagnet, and the electromagnetic stress gave an outward pressure in the ring HTSC, which is the case for the ring HTSC for the cryoundulator plus. The result is shown in figure 13 with dotted line and empty circle. The field by the electromagnet (abscissa) is shown by an absolute value of variation from the initial value (2.0 T). At the initial condition, there is an offset around 0.2 T, which is brought by magnetization of the permendur pole piece. Except the offset, we can find little difference between the measurements with the two different initial conditions. We can conclude from these facts that the pole piece insertion combined with resin impregnation significantly reinforces the ring HTSC and improves its mechanical properties.

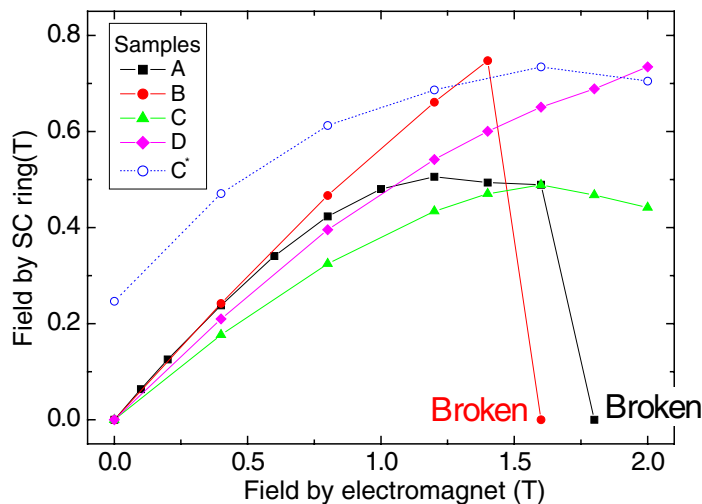


Figure 13. Summary of the experiments for the samples A–D. The samples A and B were broken at the external field of 1.8 and 1.6 T, respectively, while the samples C and D survived even after application of 2.0 T, the strongest field that can be applied by the electromagnet used in the experiment. The dotted blue line shows the result of the sample C with the different initial condition. Refer to the text.

5.4. Discussion

It should be noted that the B_{ext} value of 1.6 T at which the sample B was broken is lower than that for the sample A (1.8 T). Has the resin impregnation weakened the mechanical property of the ring HTSC? The answer is no. As found in figure 12, B_{sc} for the sample B reached 0.9 T at $B_{\text{ext}} = 1.4$ T, which is higher than the saturated value of B_{sc} for the sample A (0.50 T). The electromagnetic stress is roughly estimated by the product of B_{ext} and the persistent current in the ring HTSC. The latter is proportional to B_{sc} , thus we should compare the value $B_{\text{ext}} B_{\text{sc}}$. Now we can conclude that the tensile strength of the sample B was roughly 50% higher than that of the sample A, showing the effectiveness of resin impregnation.

Comparing the results of the experiments using the samples C and D having the same structure and method for reinforcement, we find a large discrepancy in magnetic performance, i.e., the critical current density. Needless to say, such discrepancy results in bad uniformity of the peak field of the undulator and thus worse phase errors, which may be another technical challenge to be overcome for realization of the cryoundulator plus. Especially, we have a lot of improvements to be made to the manufacturing process of HTSC samples.

6. Summary and outlook

The current status of R&D towards realization of the CPMU concept have been described. The pure- and hybrid-type CPMUs can be the major insertion device in the 3rd generation SR facilities for the next decade thanks to its simple concept. However, we should take care of a lot of things in construction of a real device. For example, an ‘*in-situ*’ field measurement system, or an apparatus to measure the magnetic field distribution of the magnet arrays inside the vacuum

chamber, should be developed. The real gap, i.e., the actual distance between the top and bottom magnet arrays, should be monitored during operation under a highly radioactive environment such as the accelerator tunnel. In addition, the monitoring systems should be ultra high vacuum (UHV) compatible. It is worth noting that these objects are common to development of IVUs for x-ray free electron lasers that should satisfy stringent specifications on magnetic performances.

Acknowledgments

We thank Drs H S Lee, D E Kim and C W Chung of Pohang Light Source for the radiation damage study on PMs.

References

- [1] Bazin M, Farge Y, Lemonnier M, Perot J and Petroff Y 1980 *Nucl. Instrum. Methods* **172** 61
- [2] Halbach K, Chin J, Hoyer E, Winick H, Cronin R, Yang J and Zambre Y 1981 *Bull. Am. Phys. Soc.* **26** 150
- [3] Hezel T, Krevet B, Moser H O, Rossmannith J A, Rossmannith R and Schneider T 1998 *J. Synchrotron Radiat.* **5** 448
- [4] Yamamoto S, Shioya T, Hara M, Kitamura H, Zhang X W, Mochizuki T, Sugiyama H and Ando M 1992 *Rev. Sci. Instrum.* **63** 400
- [5] Hara T, Tanaka T, Tanabe T, Marechal X M, Okada S and Kitamura H 1998 *J. Synchrotron Radiat.* **5** 403
- [6] Stefan P M, Krinsky S, Rakowsky G, Solomon L, Lynch D, Tanabe T and Kitamura H 1998 *Nucl. Instrum. Methods A* **412** 161
- [7] Kitamura H 2000 *J. Synchrotron Radiat.* **7** 121
- [8] Sagawa M, Hirose S, Otani Y, Miyajima H and Chikazumi S 1987 *J. Magn. Magn. Mater.* **70** 316
- [9] Kubsky S, Dolling D, Geisler A, Hobl A, Klein U, Krischel D, Moser H O, Rossmannith R and Chouhan S 2004 *AIP Conf. Proc.* **705** 223
- [10] Hara T, Tanaka T, Kitamura H, Bizen T, Marechal X, Seike T, Kohda T and Matsuura Y 2004 *Phys. Rev. ST-AB* **7** 050702
- [11] Sagawa M, Fujimura S, Yamamoto H, Matsuura Y and Hiraga K 1984 *IEEE Trans. Magn.* **20** 1584
- [12] Tanaka T, Hara T, Kitamura H, Tsuru R, Bizen T, Marechal X and Seike T 2004 *Phys. Rev. ST-AB* **7** 090704
- [13] Nariki S, Sakai N and Murakami M 2000 *Physica C* **341–8** 2409
- [14] Tomita M, Murakami M, Sawa K and Tachi Y 2001 *Physica C* **357–60** 690
- [15] Tomita M and Murakami M 2003 *Nature* **421** 517
- [16] Ikuta H, Ikeda S, Mase A, Yoshikawa M, Yanagi Y, Itoh Y, Oka T and Mizutani U 1998 *Appl. Supercond.* **6** 109
- [17] Muralidhar M, Sakai N, Jirsa M, Murakami M and Koshizuka N 2003 *Supercond. Sci. Technol.* **16** L46
- [18] Bizen T, Tanaka T, Asano Y, Kim D E, Bak J S, Lee H S and Kitamura H 2001 *Nucl. Instrum. Methods A* **467** 185
- [19] Tanaka T, Hara T, Tsuru R, Iwaki D, Bizen T, Marechal X, Seike T and Kitamura H 2006 *Supercond. Sci. Technol.* **19** S438